

Article

Genomewide m⁶A Mapping Uncovers Dynamic Changes in the m⁶A Epitranscriptome of Cisplatin-Treated Apoptotic HeLa Cells

Azime Akçaöz Alasar , Özge Tüncel , Ayşe Bengisu Gelmez, Buket Sağlam, İpek Erdoğan Vatansever  and Bünyamin Akgül * 

Noncoding RNA Laboratory, Department of Molecular Biology and Genetics, İzmir Institute of Technology, 35430 Urla İzmir, Turkey

* Correspondence: bunyaminakgul@iyte.edu.tr; Tel.: +011-90-232-7507316; Fax: +011-90-232-7507302

Abstract: Cisplatin (CP), which is a conventional cancer chemotherapeutic drug, induces apoptosis by modulating a diverse array of gene regulatory mechanisms. However, cisplatin-mediated changes in the m⁶A methylome are unknown. We employed an m⁶A miCLIP-seq approach to investigate the effect of m⁶A methylation marks under cisplatin-mediated apoptotic conditions on HeLa cells. Our high-resolution approach revealed numerous m⁶A marks on 972 target mRNAs with an enrichment on 132 apoptotic mRNAs. We tracked the fate of differentially methylated candidate mRNAs under *METTL3* knockdown and cisplatin treatment conditions. Polysome profile analyses revealed perturbations in the translational efficiency of *PMAIP1* and *PHLDA1* transcripts. Congruently, *PMAIP1* amounts were dependent on *METTL3*. Additionally, cisplatin-mediated apoptosis was sensitized by *METTL3* knockdown. These results suggest that apoptotic pathways are modulated by m⁶A methylation events and that the *METTL3*–*PMAIP1* axis modulates cisplatin-mediated apoptosis in HeLa cells.

Keywords: apoptosis; cisplatin; epitranscriptomics; m⁶A; HeLa



Citation: Alasar, A.A.; Tüncel, Ö.; Gelmez, A.B.; Sağlam, B.; Vatansever, İ.E.; Akgül, B. Genomewide m⁶A Mapping Uncovers Dynamic Changes in the m⁶A Epitranscriptome of Cisplatin-Treated Apoptotic HeLa Cells. *Cells* **2022**, *11*, 3905. <https://doi.org/10.3390/cells11233905>

Academic Editors: Patrice X. Petit and Gautam Sethi

Received: 24 July 2022

Accepted: 28 November 2022

Published: 2 December 2022

Publisher's Note: MDPI stays neutral with regard to jurisdictional claims in published maps and institutional affiliations.



Copyright: © 2022 by the authors. Licensee MDPI, Basel, Switzerland. This article is an open access article distributed under the terms and conditions of the Creative Commons Attribution (CC BY) license (<https://creativecommons.org/licenses/by/4.0/>).

1. Introduction

Apoptosis is a type of programmed cell death that is required to maintain the delicate balance between survival and cell death as part of cell and tissue homeostasis. Characterized by cytoplasmic shrinkage, chromatin condensation, nuclear fragmentation, and apoptotic bodies, it is highly useful in eliminating damaged or unneeded cells without generating an inflammatory response [1]. Thus, apoptotic processes are targeted by various chemotherapeutic drugs. For example, cisplatin induces apoptosis in cancer cells by inducing DNA lesions through intra- and inter-strand crosslinks in DNA [2,3]. DNA lesions interfere with proper DNA replication and transcription, leading to the activation of DNA-damage response (DDR) and p53. p53 then transcriptionally coordinates the expression of genes that primarily trigger the intrinsic pathway of apoptosis as well as the extrinsic pathway [4]. However, the efficacy of drugs plummets dramatically due to drug resistance, which constitutes a major challenge in clinics for the proper treatment of cancer patients. It is therefore imperative to understand the molecular mechanism of cisplatin-induced apoptosis to develop better strategies against drug resistance.

In an analogy to DNA and proteins, the chemical composition of RNA is modified co- or post-transcriptionally through epitranscriptomic mechanisms that play a vital role in the fate of modified RNAs. Of the existing 170 different types of epitranscriptomic modifications, the N⁶-methyladenosine (m⁶A) modification is the most abundant one with the presence of 0.1–0.4% of all adenosines in cellular RNAs [5]. Antibody-based enrichment coupled with high-throughput sequencing has uncovered m⁶A-methylated peaks not only on abundant tRNAs and rRNAs, but also on mRNAs [6,7]. Cell- and tissue-specific

m⁶A modifications on mRNAs modulate a diverse array of cellular processes in health and disease. The emerging evidence suggests that proteins and enzymes that orchestrate cellular m⁶A dynamics control apoptosis under various cellular settings. For example, depletion of *METTL3* leads to an increase in the rate of apoptosis by reducing the translation of *MYC*, *BCL2* and *PTEN* in leukemia cells or by *BCL2* translation reduction in breast cancer cells [8,9]. The demethylase *FTO*, on the other hand, suppresses the rate of apoptosis in human acute myeloid leukemia cells [10]. There are also reports on the modulatory effect of m⁶A reader proteins, such as *IGF2BP1*, on apoptosis [11]. However, a complete m⁶A methylome of mRNAs under apoptotic conditions has not yet been reported.

We used cisplatin, a universal cancer chemotherapeutic drug, as an inducer of apoptosis to profile m⁶A mRNA methylome in HeLa cells. Our analyses identified differential m⁶A methylation of 972 mRNAs. Interestingly, 132 of m⁶A-methylated mRNAs are associated with apoptosis as revealed by gene ontology analyses. Further analyses showed that cisplatin-induced m⁶A marks do not change the abundance of candidate mRNAs tested. However, we detected changes in the translational efficiencies of differentially methylated candidate mRNAs as revealed by polysome profiling. This observation was further supported by a corresponding increase in the protein amount, suggesting a potential role for the *METTL3*–*PMAIP1* axis in apoptosis.

2. Materials and Methods

2.1. Cell Culture, Drug Treatments and Analysis of Apoptosis

HeLa cells, purchased from DSMZ GmbH (Leibniz, Germany), and an ME-180 (HTB-33) cell line, purchased from ATCC (Manassas, VA, USA), were cultured in RPMI 1640 (Gibco, ThermoFischer, Waltham, MA, USA) and McCoy's 5A (Lonza, Switzerland) supplemented with 2 mM L-glutamine, 10% fetal bovine serum (FBS) (Gibco, ThermoFischer, Waltham, MA, USA) in a humidified atmosphere of 5% CO₂ at 37 °C. Cisplatin (Santa Cruz Biotechnology, Dallas, TX, USA) treatments were carried out in triplicates essentially as described previously [12]. 0.1% (*v/v*) DMSO was used as a negative control for cisplatin. Treated cells were trypsinized by 1X Trypsin-EDTA (Gibco, ThermoFischer, Waltham, MA, USA) and washed in 1X cold PBS (Gibco, ThermoFischer, Waltham, MA, USA). Cell pellets were stained with Annexin V-PE (BD Biosciences, Franklin Lakes, NJ, USA) and 7AAD (BD Biosciences, Franklin Lakes, NJ, USA) in the presence of 1X Annexin binding buffer (BD Biosciences, Franklin Lakes, NJ, USA) followed by incubation at room temperature for 15 min in the dark. The rates of Annexin V and/or 7AAD-positive cells were quantified by a FACSCanto flow cytometer (BD Biosciences, Franklin Lakes, NJ, USA).

2.2. Construction of Overexpression Vector and Cell Transfection

METTL3 cDNA was amplified by Q5[®] High-Fidelity DNA Polymerase (New England Biolabs, Ipswich, MA, USA) with primers harboring a *NheI*-*NotI* restriction site (Table 1, *METTL3*-OE). The 1743-bp PCR product was cloned into pcDNA3.1+ plasmid to obtain pcDNA3.1(+)+*METTL3*. The sequence of the insert was verified by Sanger sequencing. The pcDNA3.1(+) was used as the negative control. Plasmids were isolated using an endotoxin-free plasmid isolation kit (Macherey-Nagel, Dueren, Germany). A total of 75,000 cells/well HeLa cells were seeded in 6-well plates. After overnight incubation, cells were transfected with 1500 ng DNA/well using the Fugene HD transfection reagent (Promega, Madison, WI, USA) in a 2-mL final volume. Media was changed 1 h post-transfection in overexpression experiments.

Table 1. The list of primers used in qPCR analyses. OE, overexpression primers.

Genes	Forward 5'-3'	Reverse 5'-3'
METTL3	AGATGGGGTAGAAAGCCTCCT	TGGTCAGCATAGGTTACAAGAGT
METTL14	GAGTGTGTTTACGAAAATGGGGT	CCGTCTGTGCTACGCTTCA
WTAP	TTGTAATGCGACTAGCAACCAA	GCTGGGTCTACCATTGTTGATCT
RBM15	AAGATGGCGGCGTGCGGTTCCGCTGTG	AAGTTCACAAAGGCTACCCGCTCATCC
FTO	CTTCACCAAGGAGACTGCTATTTT	CAAGGTTCTGTGTGAGCACTCTG
ALKBH5	TCCAGTTCAAGCCTATTTCG	CATCTAATCTTGTCTTCCCTGAG
YTHDF1	TAAGGAAATCCAATGGACGG	TTTGAGCCCTACCTTACTGGA
YTHDF2	CCTTAGGTGGAGCCATGATTG	TCTGTGCTACCCAATTCAGT
YTHDF3	TGACAACAAACCGGTTACCA	TGTTTCTATTTCTCTCCCTACGC
YTHDC1	TCAGGAGTTCGCCGAGATGTGT	AGGATGGTGTGGAGGTGTGTCC
YTHDC2	GTGTCTGGACCCCATCTTA	CCCATCACTTCGTGCTTTTT
IGF2BP1	TAGTACCAAGAGACCAGACCC	GATTTCTGCCCGTTGTTGTC
IGF2BP2	ATCGTCAGAATTATCGGGCA	GCGTTTGGTCTCATTCTGTC
IGF2BP3	AGACACCTGATGAGAATGACC	GTTTCTGAGCCTTACTTCC
PRRC2A	AGGGCAAGTCCTTAGAGATCC	TTCAGGCTTGAAGGTTGGC
FMR1	CAGGGCTGAAGAGAAGATGG	ACAGGAGGTGGGAATCTGA
HNRNPA2B1	AGCTTTGAAACCACAGAAGAA	TTGATCTTTTGTTCAGGA
HNRNPC	TAAGGAAATCCAATGGACGG	TTTGAGCCCTACCTTACTGGA
HNRNPG	TAAGGAAATCCAATGGACGG	TTTGAGCCCTACCTTACTGGA
PHLDA1	CTTCACTGTGGTGTGCGCAGAG	CCTGACGATTCTTGTACTGCACC
PMAIP1	CTCTGTAGCTGAGTGGGCG	CGGAAGTTCAGTTGTCTCCA
PIDD1	TGTTTCGAGGGCGAAGGTTT	TCCAGAGTGGTGGTCACGTA
TRAP1	CAGGGTTCCTTCCAAACA	TGGAGATCAGCTCCCCTATAA
METTL3-OE	CTAGCTAGCATGTCGGACACGTGGA	CTAGCGGCCGCTATAAATTCTTAGG
GAPDH	ACTCCTCCACCTTTGACGC	GCTGTAGCCAAATTCGTTGTC

0.6×10^6 HeLa cells were seeded into 10 cm dishes (Sarstedt, Nümbrecht, Germany) and incubated overnight prior to transfection with 25 nM non-target pool (si-NC) or METTL3 siRNA (si-METTL3) (Dharmacon, Lafayette, CO, USA). DharmaFECT transfection reagent was mixed with siRNAs in a ratio of 2:1 (*v/v*) in an 800- μ L serum-free medium and incubated for 5 min at room temperature. The DharmaFECT solution was added into the siRNA tube and incubated for 20 min at room temperature. The mixture was then combined with an 8-mL medium by gently dropping over cells.

2.3. Total RNA Isolation and qPCR

Total RNA isolation was performed using TRIzolTM reagent (Invitrogen, ThermoFisher, Waltham, MA, USA) according to the manufacturer's protocol. Trace DNA contamination was eliminated by treating RNAs with TURBO DNA-freeTM kit (ThermoFisher Scientific, Waltham, MA, USA) according to the manufacturer's instructions.

For qPCR analyses, reverse transcription was conducted with RevertAid first strand cDNA synthesis kit according to the manufacturer's instructions (ThermoFisher Scientific, Waltham, MA, USA). cDNA was prepared using 2 μ g of total RNA and diluted 1:10 in nuclease-free water. qPCR reactions were set up in triplicate with GoTaq[®] qPCR Master Mix (Promega, Madison, WI, USA) and run in a Rotor-Gene Q machine (Qiagen, Hilden, Germany). The primer sequences are listed in Table 1. All reactions were incubated at 95 °C for 2 min as initial denaturation, 45 cycles of denaturation at 95 °C for 15 s and annealing at 60 °C for 1 min following a melting step. GAPDH was used to normalize the qPCR data.

2.4. m⁶A-eCLIP-seq and Bioinformatic Analysis

Three biological replicates of total RNAs isolated from DMSO (control) and cisplatin-treated HeLa cells were subjected to m⁶A-eCLIP-seq by Eclipse Bioinnovations (San Diego, CA, USA) according to the published protocols [13]. The data were deposited to the Genome Expression Omnibus (GEO) with the accession number GSE188580.

Data analysis was performed by Eclipse Bioinnovations using their standard pipeline [14]. Briefly, UMI sequences (the first 10 bases) were demultiplexed from each read by UMI-tools [15]. Quality control of reads and adaptor trimming from 3' ends was assessed by FastQC: v. 0.11.5 [16] and Cutadapt: v. 1.15 tools [17], respectively. After the removal of contaminating sequences (e.g., rRNA and/or other repetitive sequences) by UMI-tools, the remaining reads were aligned to the human GRCh38/hg38 reference genome utilizing STAR: v. 2.6.0c. Peaks of m⁶A modification (cluster of reads) were firstly pinpointed by CLIPper tool (<https://github.com/YeoLab/clipper>, accessed on 1 December 2022) [18,19] and the reproducibility of clusters among biological triplicates of each sample was determined by IDR analysis [20]. The log₂ fold change was calculated in two steps: (i) log₂ fold change in IP relative to its corresponding input for each sample, (ii) log₂ fold change in cisplatin-treated samples relative to the corresponding DMSO control, and vice versa. Further analysis for determination of crosslink sites at a single nucleotide resolution in IP-enriched samples relative to their inputs was performed by PureCLIP: v. 1.3.1 [14]. The validation of crosslink sites was evaluated through both reproducibility of m⁶A sites among three replicates and determination of the DRACH motif in which m⁶A sites tend to be situated [21]. Finally, each crosslink site was appointed to the gene and feature type based on the GENCODE Release 32 (GRCh38.p13). Further analyses of determined feature types and crosslink sites such as the relative frequency of peaks that map to each feature, Metagene Plot, Metaintron Plot, and Homer Motif analysis, were carried out by Eclipse Bioinnovation.

Differentially methylated RNAs were further interrogated by gene ontology (GO) enrichment analysis, KEGG enrichment analysis, and a Reactome pathway platform (the Gene Ontology Consortium, 2019, [22]).

2.5. Western Blotting

Total protein was extracted from cells using 1X RIPA buffer (Cell Signaling Technology, Danvers, MA, USA). Subsequently, 25 µg total protein extract was fractionated on a 10% SDS-PAGE and transferred onto PVDF membranes (ThermoFisher Scientific, Waltham, MA, USA). The membrane was blocked with 5% non-fat dry milk in 0.2% Tween-20 in Tris-buffered saline for 1 h at room temperature. The primary antibodies for *METTL3*, *METTL14*, *FTO*, *RBM15*, *PMAIP1*, *Caspase-9*, *Caspase-3* and *β-actin* (Cell Signaling Technology, Danvers, MA, USA) and secondary antibodies were used in 1:1000 and 1:10,000 dilution, respectively. The chemiluminescent signals were quantitated by the ImageJ program where each signal was normalized to β-actin.

2.6. Polysome Analysis

Polysome profiling was performed according to a published procedure [23]. Following centrifugation at 1200 RPM for 10 min, the cells were homogenized in lysis buffer [100 mM NaCl, 10 mM MgCl₂, 30 mM Tris-HCl (pH 7), 1% Triton X-100, 1% NaDOC, 100 µg/mL cycloheximide (Applichem, Darmstadt, Germany) and 30 U/mL RNase Inhibitor (Promega, Madison, WI, USA)]. The cell pellets were sheared to homogenization by passing the lysate through a 26 G needle at least 15 times and incubated on ice for 8 min. The lysates were then centrifuged at 12,000× g at 4 °C for 8 min. The supernatants were layered over 5–70% (*w/v*) sucrose gradients [100 mM NaCl, 10 mM MgCl₂, 30 mM Tris-HCl (pH 7.0), 200 U RNase inhibitor (Promega, Madison, WI, USA)] prepared by using an ISCO Teledyne (Lincoln, NE, USA) density gradient fractionation system and centrifuged at 27,000 RPM for 2 h 55 min at 4 °C in a Beckman SW28 rotor (Beckman Coulter, Brea, CA, USA). Fractions were collected using the ISCO Teledyne density gradient fractionation system while reading absorbance at A₂₅₄. Fractions were pooled as mRNP, monosomal, light and heavy polysomal sub-groups based on A₂₅₄ readings. The total RNA was phenol-extracted from fractions by using phenol-chloroform-isoamyl alcohol (25:24:1) (Applichem, Darmstadt, Germany).

3. Results

3.1. Cisplatin Regulates the Expression of the m⁶A Methylation Machinery

Cisplatin is a cancer chemotherapeutic drug that is widely used as a universal inducer of apoptosis [24]. We reported previously that cisplatin at a concentration of 80 μ M is sufficient to trigger approximately 50% of apoptosis in HeLa cells [25]. Thus, we treated HeLa cells with 80 μ M cisplatin for 16 h to attain an early apoptotic rate of 55% (Figure 1A,B). We also analyzed caspase activation for further confirmation of CP-induced apoptosis in HeLa cells. Caspase -3 and caspase -9 were cleaved upon CP treatment as a hallmark of cells undergoing apoptosis (Figure 1C). We then determined the expression levels of major genes involved in m⁶A RNA methylation to assess the impact of cisplatin on the m⁶A methylation machinery. To this extent, we examined the changes in the transcript levels of *METTL3*, *METTL14*, *WTAP*, *RBM15*, *FTO* and *ALKBH5* in cisplatin-treated HeLa cells. Interestingly, cisplatin treatment led to a 3.3- and 6.6-fold reduction in the mRNA levels of *METTL14* and *FTO*, respectively, as determined by qPCR analyses (Figure 1D). We then checked the amount of some of these key proteins. Our western blot analyses showed downregulation of METTL14 in parallel with the qPCR analyses (Figure 1E). Although we did not detect any changes in the mRNA levels of *METTL3* and *RBM15* (Figure 1D), we observed a decrease in the protein levels of RBM15 and METTL3 by 2.8- and 1.4-fold, respectively (Figure 1E).

3.2. Cisplatin Modulates Major Changes in the m⁶A RNA Methylome

Cisplatin-mediated changes in the mRNA and protein levels of key RNA methylation enzymes suggest substantial perturbations in the cellular RNA m⁶A methylome under apoptotic conditions. Therefore, we employed a genome-wide approach to identify the key RNA m⁶A methylation events in cisplatin-treated HeLa cells. To this extent, we performed an m⁶A miCLIP-seq analysis with three biological replicates of total RNAs isolated from DMSO- and cisplatin-treated HeLa cells. We normalized the changes in RNA m⁶A methylation events against transcript abundance to obtain the differentially m⁶A-methylated transcripts. Our analyses revealed changes in the m⁶A methylation pattern at 7658 adenosine residues with an average number of 12 m⁶A methylation per transcript (Supplementary Table S1). The extent of m⁶A methylation was reduced at 6236 sites while we detected induction in the m⁶A RNA methylation pattern at 1422 sites. We subsequently generated metatrain plots to interrogate the distribution of m⁶A sites throughout transcripts. We noticed an enrichment at the 5' and 3' UTRs of transcripts with increased and decreased m⁶A residues, respectively (Figure 2A,B). Additionally, down-regulated m⁶A methylation was predominantly localized to the 3' UTR and coding sequence of mRNAs, while the up-regulated m⁶A residues have homogenic distribution throughout mRNA (Figure 2C,D). To uncover which transcripts are specifically targeted by the m⁶A methylation machinery under cisplatin-induced apoptotic conditions, we carried out gene ontology analyses with differentially m⁶A-methylated transcripts (Supplementary Table S2). Positive regulation of the apoptotic signaling pathway was listed in number 2 (Supplementary Table S2). We subsequently selected the genes associated with apoptosis (Supplementary Table S3). Strikingly, as many as 132 genes associated with apoptosis were subjected to differential m⁶A methylation (Figure 2E, Supplementary Table S3). We selected differential m⁶A methylation on four candidate mRNAs, namely *PHLDA1*, *PIDD1*, *PMAIP1* and *TRAP1*, all of which have been reported to be key players in the modulation of apoptosis [4,26–30]. An IGV screenshot of the methylation profile for *PMAIP1* under DMSO and CP treatment conditions ($n = 3$) is presented in Figure 2F. *PMAIP1* possesses five m⁶A residues under the control DMSO treatment condition. Under cisplatin treatment conditions, we detected only 3 m⁶A marks on *PMAIP1*. Interestingly, cisplatin treatment leads to the addition of an m⁶A mark near the 5'UTR and the removal of three m⁶A residues throughout the transcript. The resulting three m⁶A marks were upregulated 4.23-, 3.5- and 3.67-fold upon cisplatin treatment.

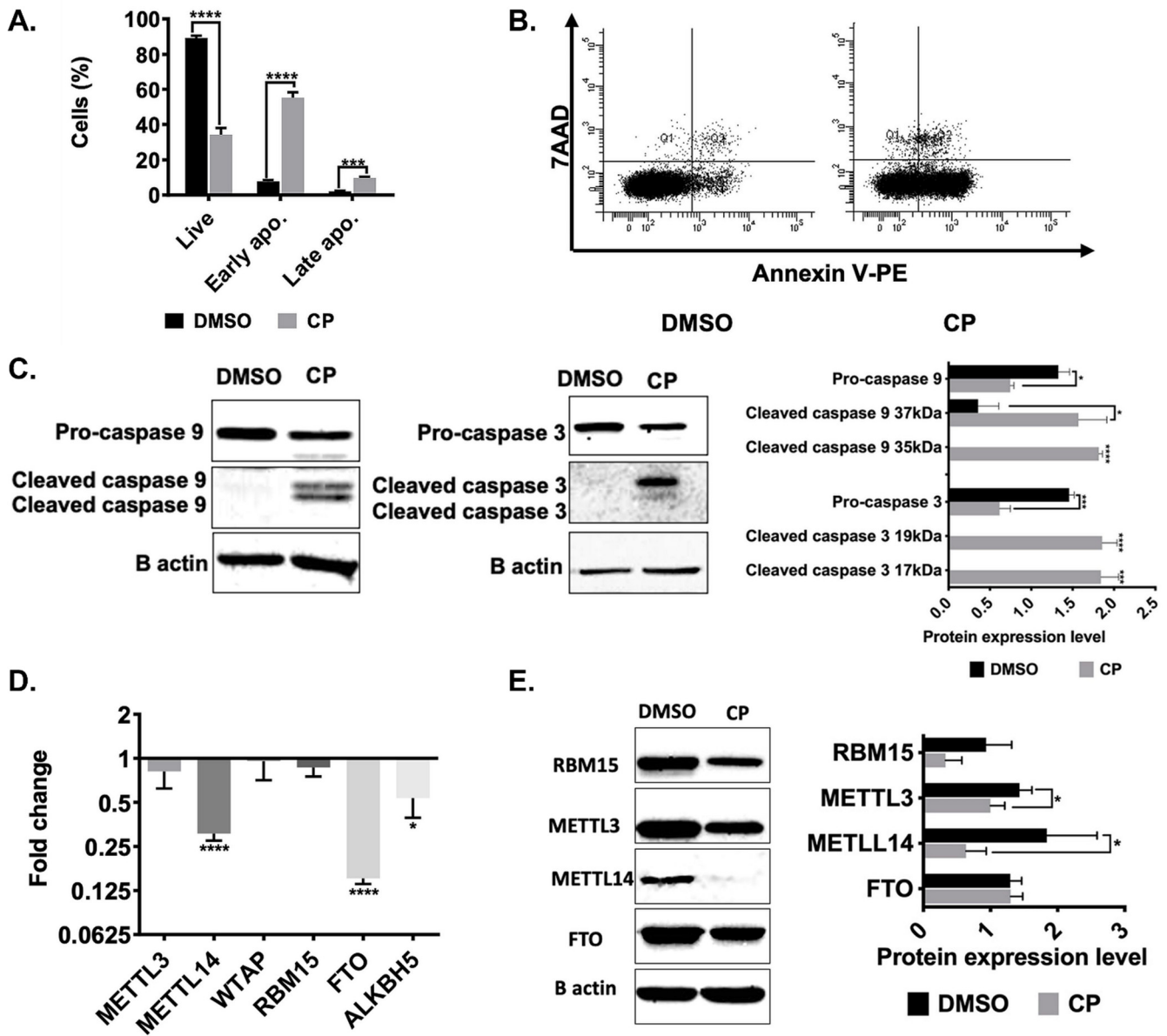


Figure 1. Expression patterns of m⁶A enzymes in cisplatin-treated HeLa cells. 1 × 10⁶ HeLa cells were treated with 80 μM cisplatin (CP) and 0.1% (v/v) DMSO for 16 h. The cells were stained with Annexin V/7AAD and examined by flow cytometry. Population distributions of DMSO- and CP-treated HeLa cells are depicted (A) Percentage of live (34%), early (55%) and late apoptosis (9.9%) and (B) Dot-blot analysis by flow cytometry after staining with Annexin V-PE and 7AAD. (C) Western blot analysis of caspase-3 and caspase-9 in HeLa cells treated with 80 μM CP and 0.1% (v/v) DMSO for 16 h. Equal amounts of total proteins (25 μg/lane) were fractionated through a 10% SDS-PAGE. (D) qPCR analysis of gene expression. Results were normalized against GAPDH. (E) Western blot analysis. Band intensities were normalized against β-actin, used as a loading control. Experiments were conducted in triplicates. *: *p* ≤ 0.05, **: *p* ≤ 0.001, ***: *p* ≤ 0.0001 by a two-tailed unpaired t-test.

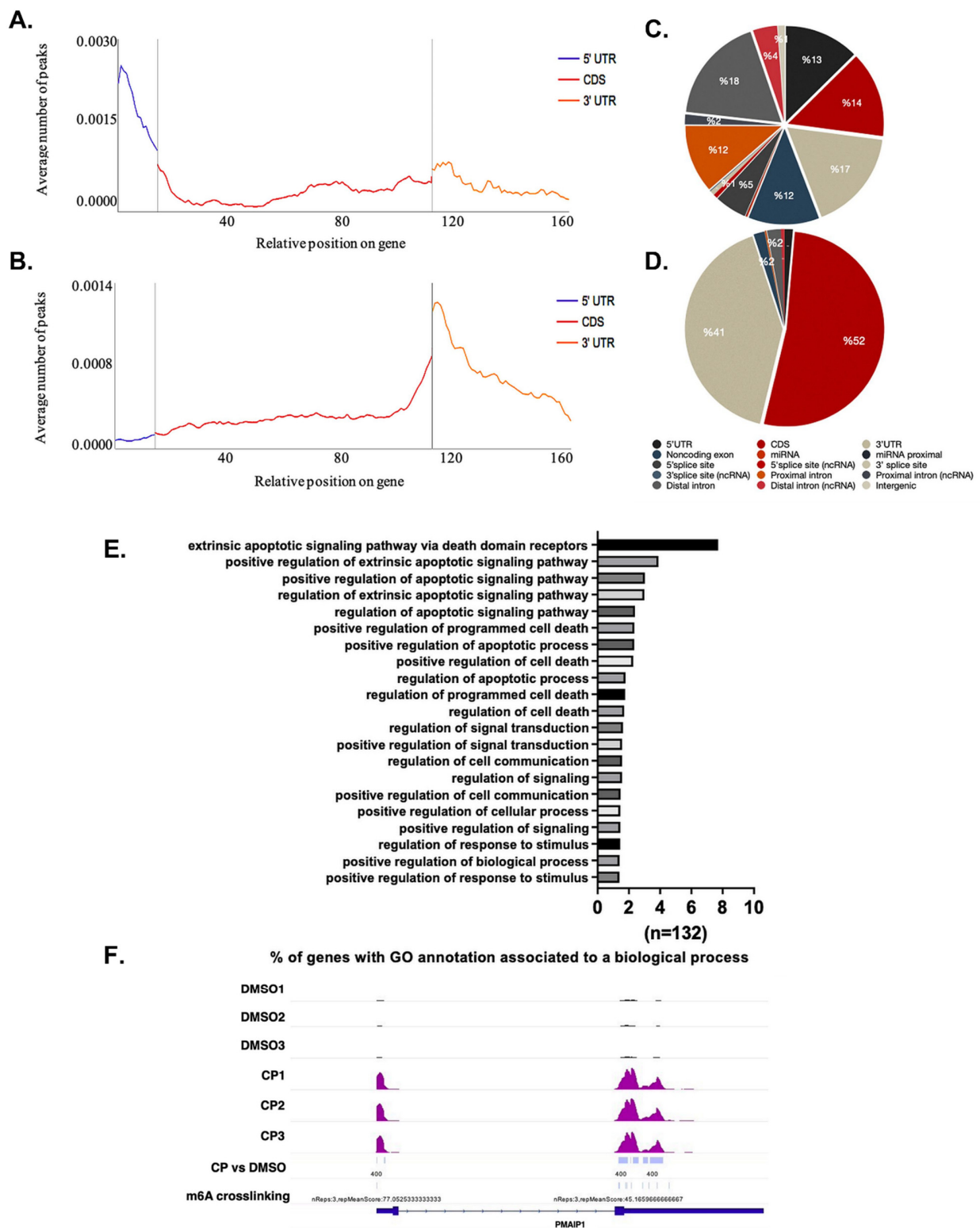


Figure 2. m⁶A RNA methylome profile of cisplatin-treated HeLa cells. The m⁶A methylome of DMSO control and CP-treated HeLa cells were obtained by miCLIP-seq as described in Materials and Methods. Distribution of upregulated (A) and downregulated (B) m⁶A peaks are shown across all transcripts. Pie chart of upregulated (C) and downregulated (D) m⁶A peaks representing their location on transcripts. Biological replicates: *n* = 3 per group. (E) Gene ontology (GO) analysis of differentially m⁶A-methylated transcripts associated with apoptosis. All biological processes were plotted having a false discovery rate (FDR) < 0.05. (F) m⁶A methylation profile of *PMAIP1*.

3.3. Cisplatin Modulates Translational Efficiency of mRNAs in a METTL3-Dependent Manner

RNA m⁶A methylation may dictate the fate of transcripts both transcriptionally and post-transcriptionally [29]. Therefore, we first examined the impact of RNA m⁶A methylation on transcript abundance in the presence or absence of cisplatin and/or *METTL3*. Although *METTL3* knockdown (Figure 3A) did not change the viability of HeLa cells in the absence of cisplatin (e.g., DMSO treatment), we observed a 3.5% decrease in the percentage of live cells and a 5.8% increase in the percentage of early apoptotic cells (Figure 3B, $p < 0.05$), suggesting that *METTL3* knockdown probably sensitizes HeLa cells to cisplatin-induced apoptosis. Before we investigated the cisplatin inducibility of candidate genes in the absence of *METTL3*, we first interrogated their abundance in cisplatin-treated and *METTL3* knockdown HeLa cells separately. Based on our qPCR analyses, cisplatin treatment led to a 14.3-, 12.1- and 3.2-fold increase in the transcript amount of *PHLDA1*, *PMAIP1* and *PIDD1*, respectively (Figure 3C). On the other hand, *METTL3* knockdown did not have a major impact on the transcript abundance of any of the candidates tested (Figure 3D). We then measured the mRNA amounts in DMSO- and cisplatin-treated HeLa cells following the knockdown of *METTL3*. Similarly, no major effects were observed on transcript abundance (Figure 3E,F).

As the transcript abundance of candidate genes does not appear to be influenced by *METTL3* knockdown in cisplatin-treated HeLa cells, we hypothesized that RNA m⁶A methylation could be critical for translational efficiency of target RNAs under cisplatin-induced apoptotic conditions. Thus, we examined the polysome profiles of cells under various conditions as the association of mRNAs with polysomes is a good indicator of their translational efficiency [30]. The knockdown of *METTL3* did not appear to have a discernible effect on the overall polysome profile (Figure 4A; Supplementary Figure S1), excluding any global effect on translation. We then investigated the association of individual mRNAs with actively translating polysomes. To this extent, we first fractionated the cytoplasmic extracts of HeLa cells into four major fractions (1) mRNP fraction composed primarily of non-translated ribonucleoproteins; (2) monosome constituting mRNAs associated with a single ribosome; (3) light polysome that contains mRNAs associated with up to 3 ribosomes; and (4) heavy polysome that contains mRNAs with more than 3 ribosomes. We performed qPCR analyses with phenol-extracted total RNAs from each fraction. Our results exhibited almost no changes in the translational efficiency of *PHLDA1*, *PIDD1*, *PMAIP1* and *TRAP1* mRNAs upon *METTL3* knockdown (Figure 4B–E). We then examined the translational efficiency of these transcripts in cisplatin-treated HeLa cells upon the *METTL3* knockdown to interrogate the potential contribution of *METTL3* to the translational efficiency of transcripts under cisplatin-induced apoptosis. In agreement with our data in Figure 4, the treatment of HeLa cells with DMSO as a control group did not cause any changes in the sedimentation of the transcripts on sucrose gradients upon the *METTL3* knockdown (Figure 5A,B,D,F,H; Supplementary Figure S2). Interestingly, we detected CP-mediated changes in the translational efficiency of *PHLDA1* (Figure 5C, monosome, 7.1-fold, $p < 0.05$), *PMAIP1* (Figure 5E, light polysome, 14.2-fold, $p < 0.05$) and *PIDD1* (Figure 5I, mRNP, 2.4-fold, $p < 0.05$) mRNAs, but not *TRAP1* (Figure 5G). A CP-mediated increase in the translational efficiency of *PMAIP1* has caught our attention as *PMAIP1* has been reported to mediate apoptosis by inducing the intrinsic apoptotic pathway [31]. To substantiate our observation with the polysome analysis, we measured the protein amount of *PMAIP1* in CP-treated HeLa cells upon the *METTL3* knockdown. *PMAIP1* was undetectable in DMSO-treated cells. However, CP caused a sharp increase in the protein level (Figure 6A). We then examined the protein level of *PMAIP1* in *METTL3* knockdown cells upon CP treatment. Interestingly, the *METTL3* knockdown resulted in an increase in the protein level of *PMAIP1* compared to the cells transfected with the control siRNA (Figure 6A,B, 1.5-fold, $p < 0.001$). The CP-mediated increase in the protein level of *PMAIP1* in *METTL3*-knockdown cells was accompanied by a parallel increase in the amount of cleaved caspase 9 (Figure 6C). To examine whether the change in the *PMAIP1* amount is specifically due to the knockdown of *METTL3* upon CP treatment, we performed CP

treatment in HeLa cells in which *METTL3* was overexpressed. *METTL3* overexpression was able to partially rescue the change in the *PMAIP1* expression as *METTL3* overexpression resulted in a decrease in *PMAIP1* protein levels (Figure 6D).

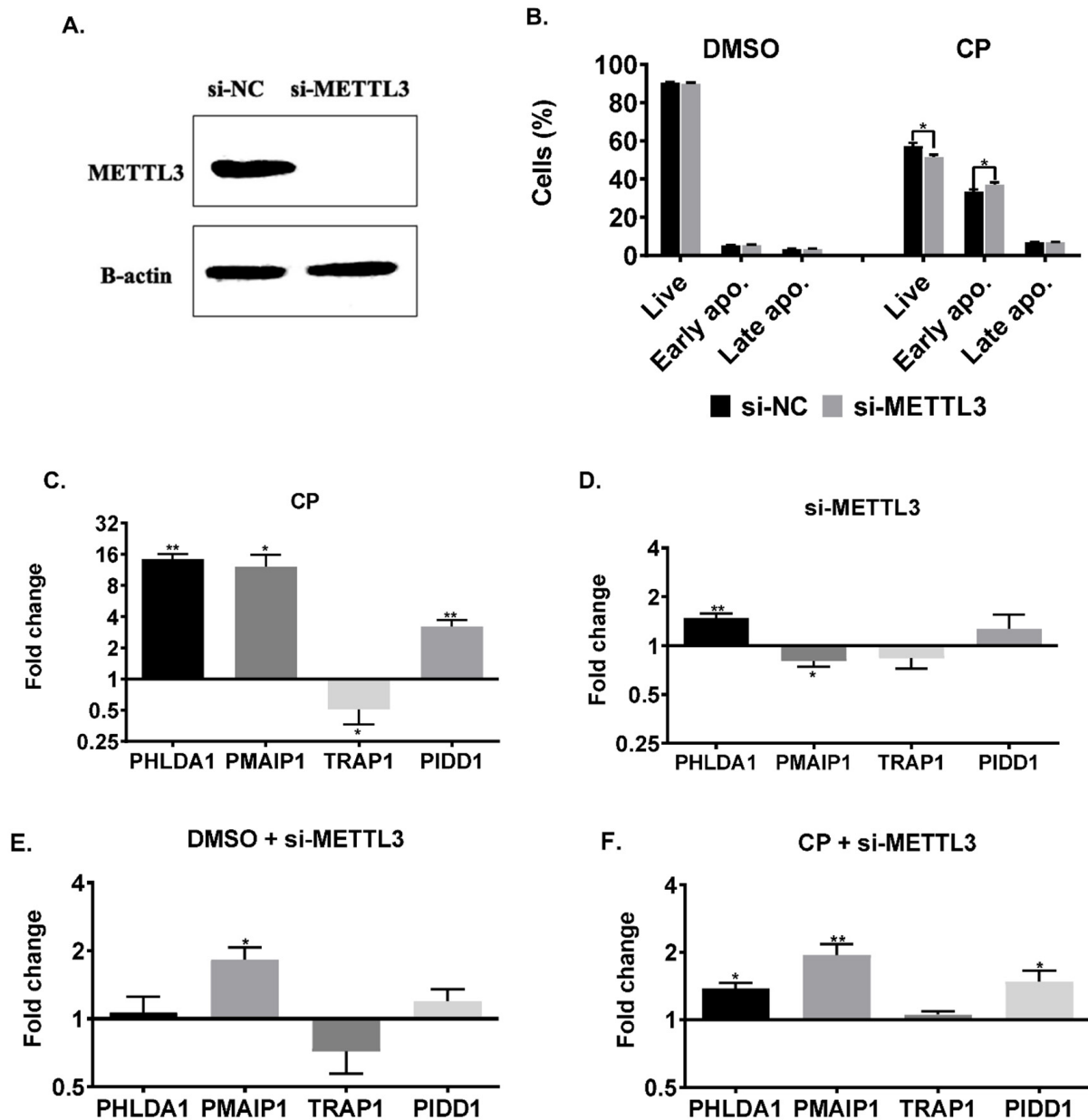


Figure 3. RNA abundance in cisplatin-treated *METTL3* knockdown HeLa cells. (A) Western blot showing *METTL3* knockdown in HeLa cells. si-NC was used as negative control. B-actin was used as loading control. (B) Apoptotic population distribution of si-NC- and si-METTL3-transfected cells followed by DMSO (0.05%)- and CP-treatment (40 μ M) for 16 h, respectively. qPCR analyses of total RNAs isolated from DMSO- and CP-treated (C), si-NC and si-METTL3-transfected cells (D), si-METTL3-transfected and DMSO-treated cells (E) and si-METTL3-transfected and CP-treated cells (F). n = 3 $p > 0.05$, * $p \leq 0.05$, ** $p \leq 0.01$ by two-tailed unpaired *t*-test.

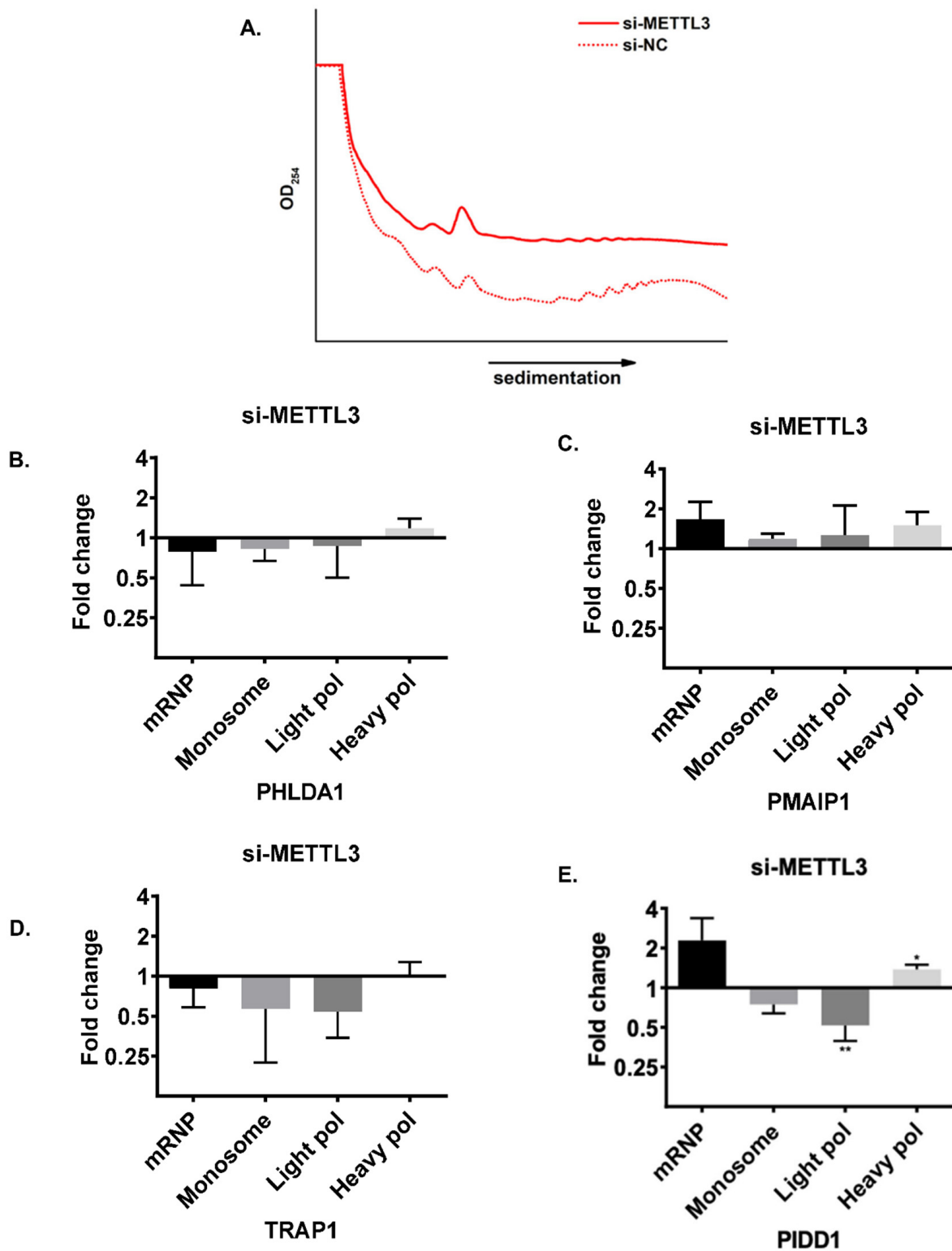


Figure 4. Polysome profiling in *METTL3* knockdown HeLa cells. Polysome profiles of cells transfected with si-METTL3 or negative siRNA (si-NC) (A). Total RNAs were phenol-extracted from each fraction collected based on the polysome profile and transcript abundance was measured by qPCR for *PHLDA1* (B), *PMAIP1* (C), *TRAP1* (D) and *PIDD1* (E). $n = 3$. $p > 0.05$, *: $p \leq 0.05$, **: $p \leq 0.01$ by two-tailed unpaired t-test.

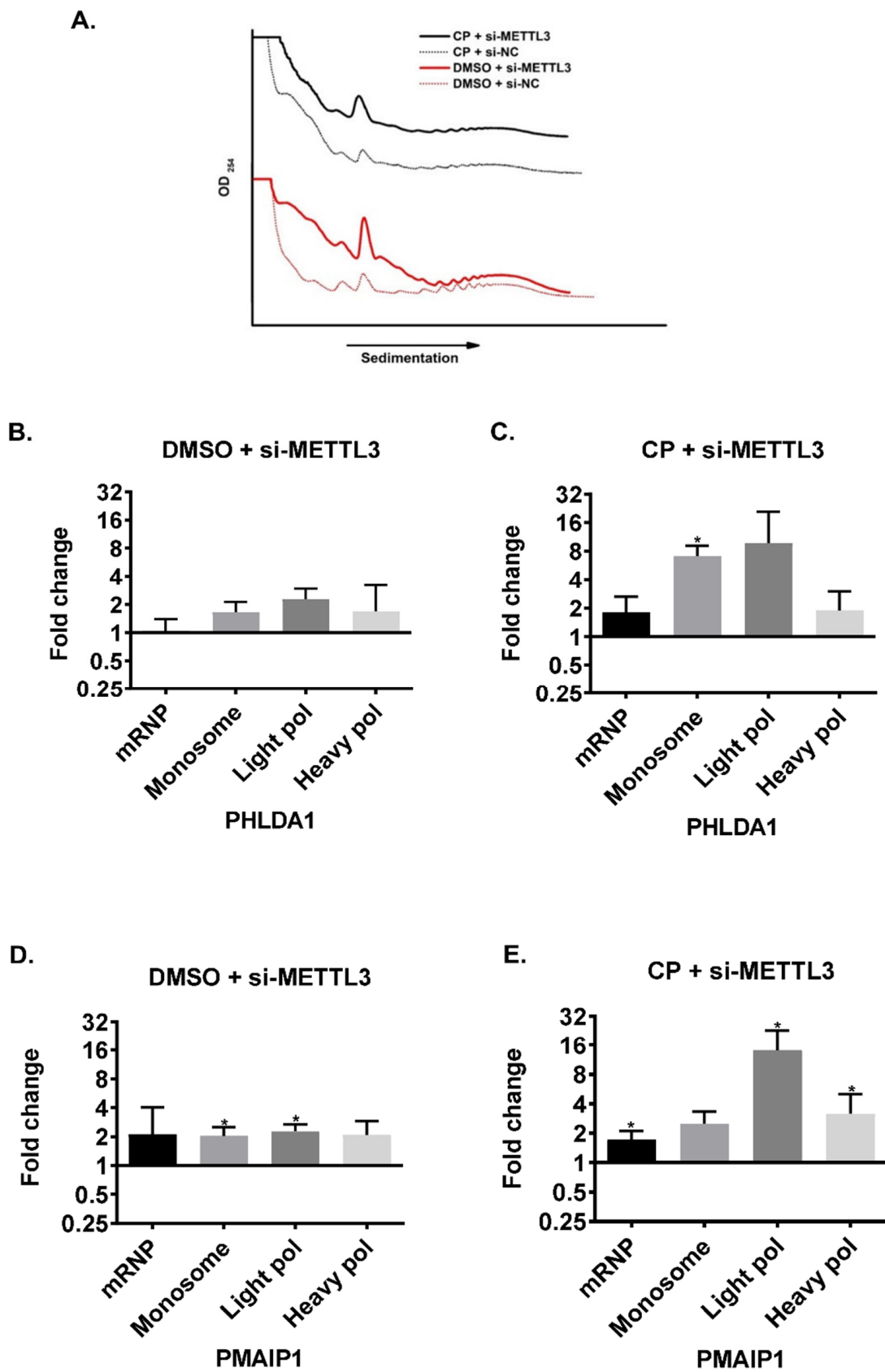


Figure 5. Cont.

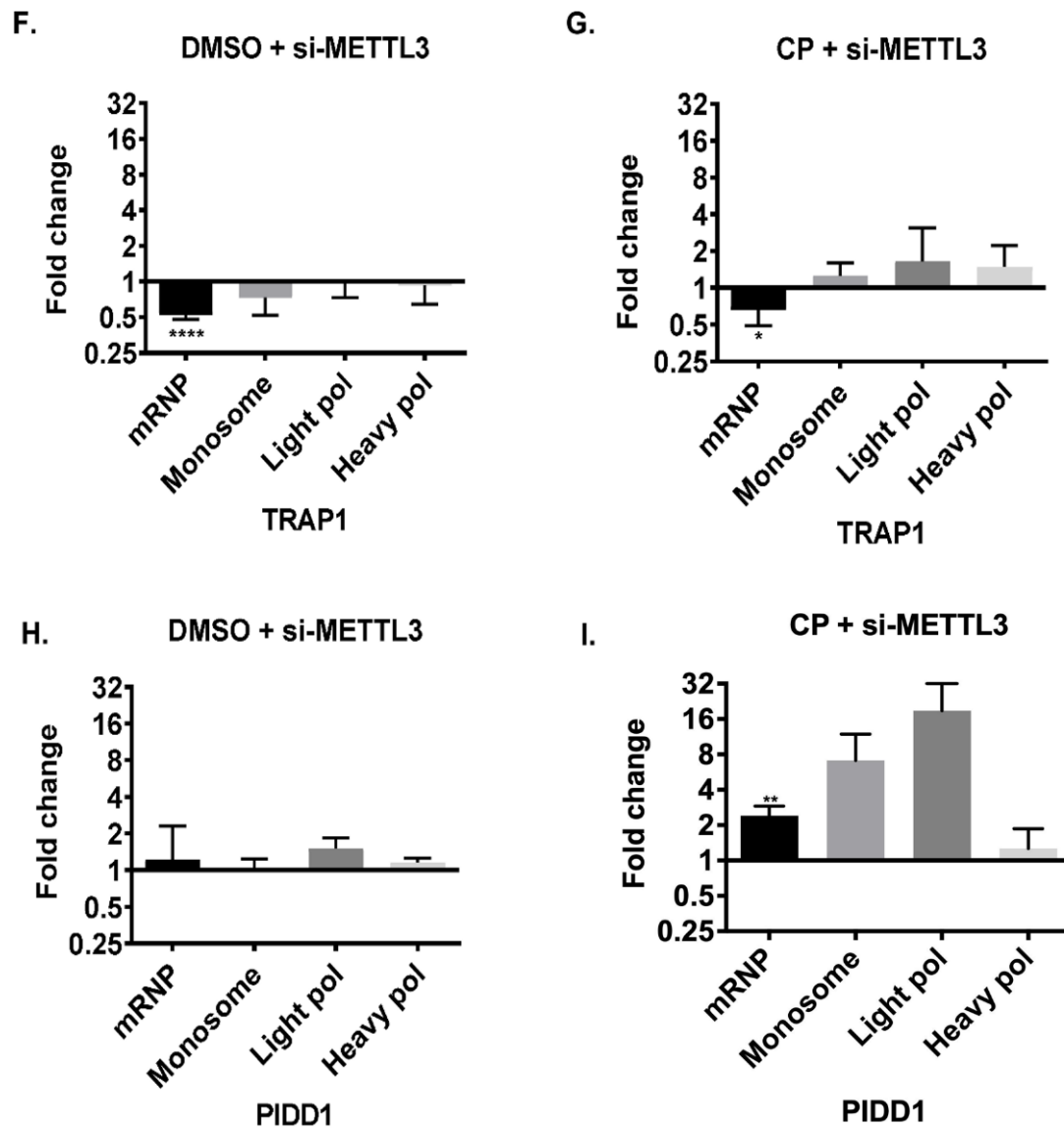


Figure 5. Polysome profiling in cisplatin-treated *METTL3* knockdown HeLa cells. Polysome profiles of cells transfected with si-*METTL3* or negative siRNA (si-NC) and treated with 40 μ M CP for 16 h (A). Total RNAs were phenol-extracted from each fraction and transcript abundance was examined by qPCR for *PHLDA1* (B,C), *PMAIP1* (D,E), *TRAP1* (F,G) and *PIDD1* (H,I) $n = 3$. *: $p \leq 0.05$, **: $p \leq 0.01$, ***: $p \leq 0.0001$ by two-tailed unpaired *t*-test.

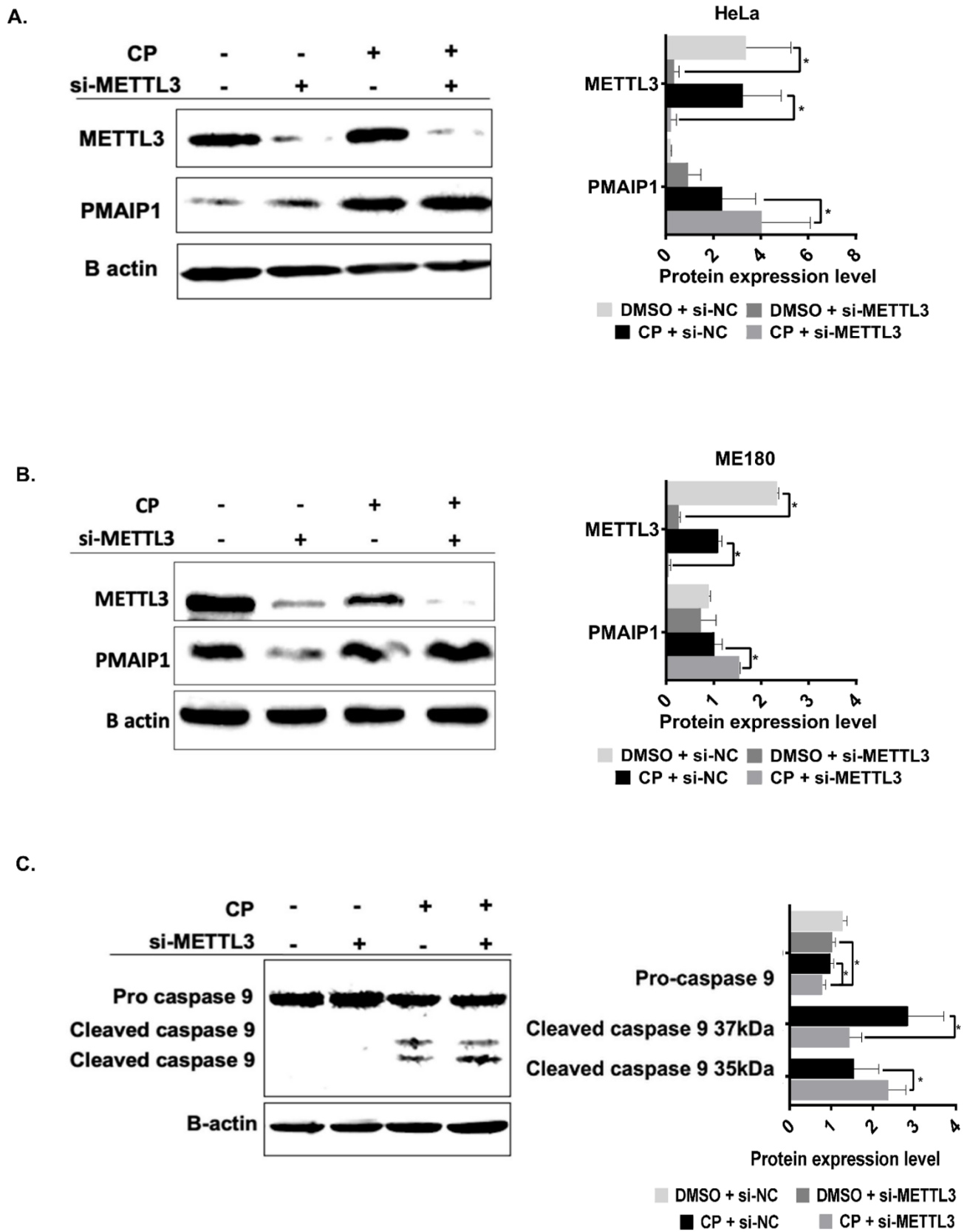


Figure 6. Cont.

D.

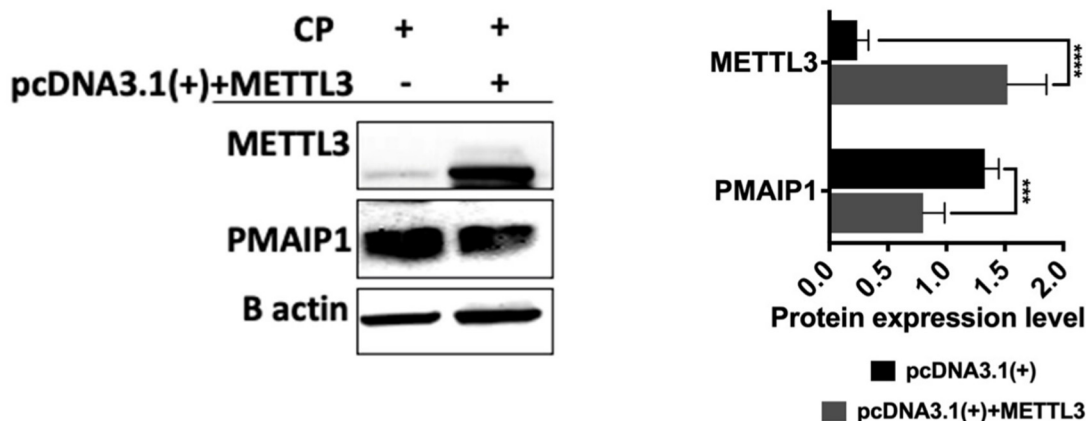


Figure 6. The *METTL3*-*PMAIP1* axis in *METTL3* knockdown and overexpressed HeLa cells. Constitutive *PMAIP1* protein expression in HeLa (A,C) and ME-180 (B) cells transfected with si-*METTL3* and treated with CP as in Figure 3. Overexpression of *METTL3* causes reduction in CP-induced *PMAIP1* (D). β -actin was used as loading control. $n = 3$ *: $p \leq 0.05$ **: $p \leq 0.001$, ***: $p \leq 0.0001$ by two-tailed unpaired *t*-test.

4. Discussion

We report for the first time that the m⁶A methylation machinery plays a fundamental role in modulating cisplatin-mediated apoptosis in HeLa cells (Figure 1). As a drug with pleiotropic effects, cisplatin induces dynamic changes in the m⁶A methylome associated not only with apoptosis but also with stress, growth, migration, etc. (Figure 2). Our genome-wide approach uncovers the fact that the *METTL3*-*PMAIP1* axis appears to modulate apoptosis through the *METTL3*-mediated changes in *PMAIP1* protein amounts (Figures 5 and 6).

METTL3 has been reported to play a role in cell death as its knockdown induces apoptosis in HepG2 cells by modulating the *P53* signaling and splicing of isoforms of *MDM2*, *FAS* and *BAX* [6]. *METTL3* was also shown to be involved in the selective recruitment of DNA polymerase to damaged DNA sites in order to orchestrate repair [32]. Additionally, there are reports on the role of ALKBH5-mediated methylation on cisplatin resistance [33,34]. Although we did not detect any change in the rate of apoptosis in *METTL3* knockdown cells, the knockdown sensitized the cells to cisplatin-induced apoptosis (Figure 3B). Our gene expression analyses in apoptotic HeLa cells also revealed major perturbations in the amounts of *METTL3*, *METTL14* and *RBM15* without any change in *FTO* (Figure 1). Although these observations clearly suggest a critical role for m⁶A methylation in coordinating different types of cell death [35], a complete m⁶A methylome profiling would be needed to gain insight into the extent of dynamic changes in the m⁶A RNA methylome under cisplatin-induced apoptotic conditions. We detected as many as 972 differentially m⁶A-methylated mRNAs, of which 132 were associated with apoptosis (Figure 2). Condition-specific enrichment of m⁶A on mRNAs has been reported previously. For example, m⁶A residues in 5' UTRs have been associated with a cap-independent translation [36]. On the other hand, m⁶A residues on coding regions (CDs) were reported to induce translation by helping resolve secondary structures [37]. We did not detect any enrichment on any specific regions of mRNAs except for a slight enrichment on the terminal part of 5' and 3' UTRs (Figure 2A).

m⁶A residues determine the fate of mRNAs at both transcriptional and posttranscriptional levels [29]. We first examined the abundance of our candidate mRNAs to probe into the impact of differential m⁶A methylation on the transcription rate and/or mRNA stability. Our qPCR analyses revealed no changes in the mRNA abundance of *PHLDA1*, *PMAIP1*, *TRAP1* and *PIDD1* (Figure 3). However, we observed a strong association between *METTL3* and translational efficiency of these mRNAs especially under cisplatin treatment conditions (Figure 5). Although *METTL3* is reported to promote translation in human cancer cells

independent of its catalytic activity and m⁶A readers [38], the *METTL3* knockdown resulted in a better association of our candidate mRNAs with polysomes, especially *PHLDA1*, *PIDD1* and *PMAIP1*, under cisplatin treatment conditions (Figure 5). It is interesting that the *METTL3* knockdown did not influence the extent of polysome association of these RNAs under control DMSO treatment (Figures 4 and 5).

PMAIP1 is a proapoptotic protein that targets MCL1 or BCL2A1 proteins for degradation [39]. As a p53-responsive gene, *PMAIP1* induces apoptosis in HeLa cells by activating caspase-9 [31]. Thus, we examined whether the enhanced translational efficiency of *PMAIP1* in *METTL3* knockdown cells results in an increase in its protein amount. Expectedly, the *METTL3* knockdown leads to an increase in the *PMAIP1* amount both in HeLa and ME-180 cells (Figure 6A,B). Additionally, we detected an elevation in the amount of cleaved caspase-9 in cisplatin-treated HeLa cells upon the *METTL3* knockdown. It is extremely interesting that the *PMAIP1* is targeted by the m⁶A machinery both transcriptionally [40] and post-transcriptionally (Figure 6). Additionally, miCLIP results showed that the *PMAIP1* has a m⁶A residue near 5'UTR in cisplatin-treated HeLa cells (Figure 7). It is interesting that cisplatin treatment leads to the addition of a m⁶A mark on one site while removing m⁶A marks on other sites. In a stress-induced translational response, mRNA containing an m⁶A modification in their 5'UTR leads to a translation via the eukaryotic initiation factor 3 (eIF3) in a cap-independent manner [36]. A high translation efficiency of the *PMAIP1* may be explained by an m⁶A residue within the 5'UTR under cisplatin treatment. Future experiments combining a depletion in m⁶A residue within the 5'UTR of *PMAIP1* and its interaction with eIF3 will provide more insight into the *PMAIP1* level in regulating the m⁶A and translation.

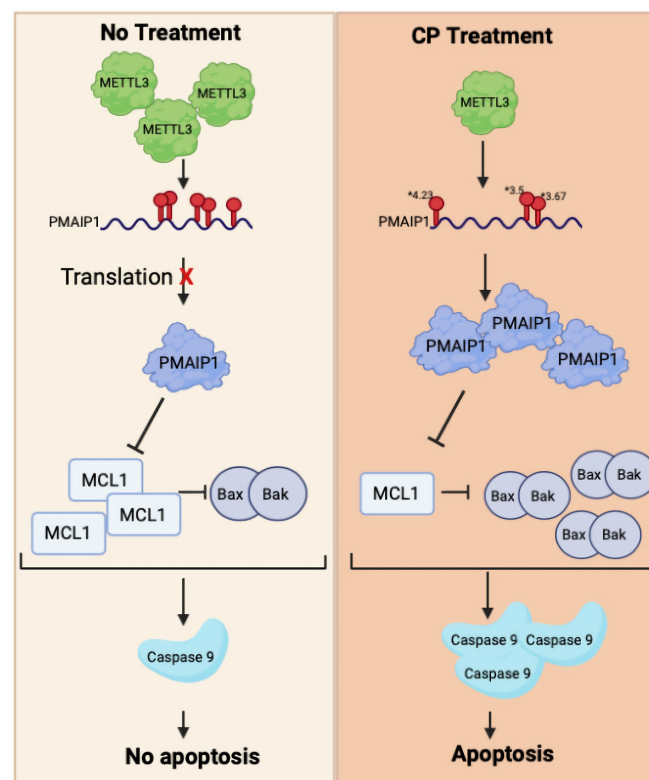


Figure 7. Working model. Under control conditions, *PMAIP1* mRNA possesses m⁶A marks at five different sites. Cisplatin treatment downregulates *METTL3* and mediates demethylation of three m⁶A residues. However, 5'UTR of *PMAIP1* is methylated and *PMAIP1* translation is enhanced. Translationally enhanced *PMAIP1* may then promote apoptosis by inhibiting MCL1 [41], suggesting a novel *METTL3*–*PMAIP1* axis that may modulate apoptosis under cisplatin treatment conditions. * Fold of induction.

Supplementary Materials: The following supporting information can be downloaded at: <https://www.mdpi.com/article/10.3390/cells11233905/s1>. Figure S1. Representative profile for area calculation (A). The numbers represent the calculated area of mRNP, monosome and polysomal volumes. Each fraction was calculated, and statistically analyzed on Graphpad (B). One of the replicates has been presented in the main manuscript. Two other replicates for si-METTL3 and si-NC pairs were illustrated in C and D. Figure S2. The calculated area of the profiles of DMSO and CP treated si-NC and si-METTL3 cells were shown as bar graphs (A). One of the replicates has been presented in the main Manuscript. The translational profiles of two other replicates were represented in B and C. Table S1: DOWNREGULATED m6A. Table S2: GEO analysis. Table S3: Differentially methylated apoptotic genes.

Author Contributions: B.A. contemplated the project. Ö.T. performed polysome experiments. A.A.A., B.S., A.B.G. and İ.E.V. performed all other experiments. A.A.A. and B.A. wrote the manuscript, Ö.T., B.S., A.B.G. and İ.E.V. read and approved the manuscript. All authors have read and agreed to the published version of the manuscript.

Funding: This study was funded by the Scientific and Technological Research Council of Turkey (TÜBİTAK) (Project No: 217Z234 to BA). A.B.G. is a recipient of a YOK 100/2000 fellowship. APC is funded by İzmir Institute of Technology.

Institutional Review Board Statement: Not applicable.

Informed Consent Statement: Not applicable.

Data Availability Statement: The data were deposited to the Genome Expression Omnibus (GEO) with the accession number GSE188580.

Acknowledgments: The authors would like to thank Dilek Telci Temeltaş for the PMAIP1 antibody. The authors would also like to thank Özgür Okur and Murat Delman for flow cytometry analyses, and BIOMER (IZTECH, Turkey) for their instrumental help.

Conflicts of Interest: The authors declare no conflict of interest.

References

1. Elmore, S. Apoptosis: A review of programmed cell death. *Toxicol. Pathol.* **2007**, *35*, 495–516. [[CrossRef](#)] [[PubMed](#)]
2. Chen, P.; Li, J.; Chen, Y.C.; Qian, H.; Chen, Y.J.; Su, J.Y.; Wu, M.; Lan, T. The functional status of DNA repair pathways determines the sensitization effect to cisplatin in non-small cell lung cancer cells. *Cell. Oncol.* **2016**, *39*, 511–522. [[CrossRef](#)] [[PubMed](#)]
3. Ming, X.; Groehler, I.A.; Michaelson-Richie, E.D.; Villalta, P.W.; Campbell, C.; Tretyakova, N.Y. Mass Spectrometry Based Proteomics Study of Cisplatin-Induced DNA–Protein Cross-Linking in Human Fibrosarcoma (HT1080) Cells. *Chem. Res. Toxicol.* **2017**, *30*, 980–995. [[CrossRef](#)]
4. Wang, J.; Thomas, H.R.; Li, Z.; Yeo, N.C.; Scott, H.E.; Dang, N.; Hossain, M.I.; Andrabi, S.A.; Parant, J.M. Puma, noxa, p53, and p63 differentially mediate stress pathway induced apoptosis. *Cell Death Dis.* **2021**, *12*, 1–11. [[CrossRef](#)] [[PubMed](#)]
5. Wei, C.-M.; Gershowitz, A.; Moss, B. Methylated nucleotides block 5' terminus of HeLa cell messenger RNA. *Cell* **1975**, *4*, 379–386. [[CrossRef](#)] [[PubMed](#)]
6. Dominissini, D.; Moshitch-Moshkovitz, S.; Schwartz, S.; Salmon-Divon, M.; Ungar, L.; Osenberg, S.; Cesarkas, K.; Jacob-Hirsch, J.; Amariglio, N.; Kupiec, M.; et al. Topology of the human and mouse m6A RNA methylomes revealed by m6A-seq. *Nature* **2012**, *485*, 201–206. [[CrossRef](#)]
7. Meyer, K.D.; Saletore, Y.; Zumbo, P.; Elemento, O.; Mason, C.E.; Jaffrey, S.R. Comprehensive Analysis of mRNA Methylation Reveals Enrichment in 3' UTRs and near Stop Codons. *Cell* **2012**, *149*, 1635–1646. [[CrossRef](#)]
8. Vu, L.P.; Pickering, B.F.; Cheng, Y.; Zaccara, S.; Nguyen, D.; Minuesa, G.; Chou, T.; Chow, A.; Saletore, Y.; Mackay, M.; et al. The N6-methyladenosine (m6A)-forming enzyme METTL3 controls myeloid differentiation of normal hematopoietic and leukemia cells. *Nat. Med.* **2017**, *23*, 1369–1376. [[CrossRef](#)]
9. Wang, H.; Xu, B.; Shi, J. N6-methyladenosine METTL3 promotes the breast cancer progression via targeting Bcl-2. *Gene* **2019**, *722*, 144076. [[CrossRef](#)]
10. Huang, Y.; Su, R.; Sheng, Y.; Dong, L.; Dong, Z.; Xu, H.; Ni, T.; Zhang, Z.S.; Zhang, T.; Li, C.; et al. Small-Molecule Targeting of Oncogenic FTO Demethylase in Acute Myeloid Leukemia. *Cancer Cell* **2019**, *35*, 677–691.e10. [[CrossRef](#)]
11. Xu, F.; Li, C.H.; Wong, C.H.; Chen, G.G.; Lai, P.B.S.; Shao, S.; Chan, S.L.; Chen, Y. Genome-Wide Screening and Functional Analysis Identifies Tumor Suppressor Long Noncoding RNAs Epigenetically Silenced in Hepatocellular Carcinoma. *Cancer Res.* **2019**, *79*, 1305–1317. [[CrossRef](#)] [[PubMed](#)]
12. Yaylak, B.; Erdogan, I.; Akgul, B. Transcriptomics Analysis of Circular RNAs Differentially Expressed in Apoptotic HeLa Cells. *Front. Genet.* **2019**, *10*, 176. [[CrossRef](#)] [[PubMed](#)]

13. Linder, B.; Grozhik, A.V.; Olarerin-George, A.O.; Meydan, C.; Mason, C.E.; Jaffrey, S.R. Single-nucleotide-resolution mapping of m6A and m6Am throughout the transcriptome. *Nat. Methods* **2015**, *12*, 767–772. [[CrossRef](#)] [[PubMed](#)]
14. Krakau, S.; Richard, H.; Marsico, A. PureCLIP: Capturing target-specific protein-RNA interaction footprints from single-nucleotide CLIP-seq data. *Genome Biol.* **2017**, *18*, 1–17. [[CrossRef](#)]
15. Smith, T.; Heger, A.; Sudbery, I. UMI-tools: Modeling sequencing errors in Unique Molecular Identifiers to improve quantification accuracy. *Genome Res.* **2017**, *27*, 491–499. [[CrossRef](#)]
16. Andrews, S.; Krueger, F.; Secondi-Pichon, A.; Biggins, F.; Wingett, S.; Fast, Q.C. A Quality Control Tool for High Throughput Sequence Data. Available online: <http://www.bioinformatics.babraham.ac.uk/projects/fastqc> (accessed on 1 December 2022).
17. Martin, M. Cutadapt removes adapter sequences from high-throughput sequencing reads. *EMBnet. J.* **2011**, *17*, 10–12. [[CrossRef](#)]
18. Yeo, G.W.; Coufal, N.G.; Liang, T.Y.; Peng, G.E.; Fu, X.D.; Gage, F.H. An RNA code for the FOX2 splicing regulator revealed by mapping RNA-protein interactions in stem cells. *Nat. Struct. Mol. Biol.* **2009**, *6*, 130–137. [[CrossRef](#)]
19. Lovci, M.T.; Ghanem, D.; Marr, H.; Arnold, J.; Gee, S.; Parra, M.; Liang, T.Y.; Stark, T.J.; Gehman, L.T.; Hoon, S.; et al. Rbfox proteins regulate alternative mRNA splicing through evolutionarily conserved RNA bridges. *Nat. Struct. Mol. Biol.* **2013**, *20*, 1434–1442. [[CrossRef](#)]
20. Li, Q.; Brown, J.B.; Huang, H.; Bickel, P.J. Measuring reproducibility of high-throughput experiments. *Ann. Appl. Stat.* **2011**, *5*, 1752–1779. [[CrossRef](#)]
21. Wang, J.; Wang, L. Deep analysis of RNA N6-adenosine methylation (m6A) patterns in human cells. *NAR Genom. Bioinform.* **2020**, *2*, lqaa007. [[CrossRef](#)]
22. Griss, J.; Viteri, G.; Sidiropoulos, K.; Nguyen, V.; Fabregat, A.; Hermjakob, H. ReactomeGSA—Efficient Multi-Omics Comparative Pathway Analysis. *Mol. Cell. Proteom.* **2020**, *19*, 2115–2125. [[CrossRef](#)] [[PubMed](#)]
23. Göktaş, Ç.; Yiğit, H.; Coşacak, M.İ.; Akgül, B. Differentially expressed tRNA-derived small RNAs co-sediment primarily with non-polysomal fractions in *Drosophila*. *Genes* **2017**, *8*, 333. [[CrossRef](#)] [[PubMed](#)]
24. Kelland, L. The resurgence of platinum-based cancer chemotherapy. *Nat. Rev. Cancer* **2007**, *7*, 573–584. [[CrossRef](#)] [[PubMed](#)]
25. Gurer, D.C.; Erdogan, I.; Ahmadov, U.; Basol, M.; Sweef, O.; Cakan-Akdogan, G.; Akgül, B. Transcriptomics Profiling Identifies Cisplatin-Inducible Death Receptor 5 Antisense Long Non-coding RNA as a Modulator of Proliferation and Metastasis in HeLa Cells. *Front. Cell Dev. Biol.* **2021**, *9*, 1–13. [[CrossRef](#)]
26. Murata, T.; Sato, T.; Kamoda, T.; Moriyama, H.; Kumazawa, Y.; Hanada, N. Differential susceptibility to hydrogen sulfide-induced apoptosis between PHLDA1-overexpressing oral cancer cell lines and oral keratinocytes: Role of PHLDA1 as an apoptosis suppressor. *Exp. Cell Res.* **2014**, *320*, 247–257. [[CrossRef](#)]
27. Sladky, V.; Schuler, F.; Fava, L.; Villunger, A. The resurrection of the PIDDosome—Emerging roles in the DNA-damage response and centrosome surveillance. *J. Cell Sci.* **2017**, *130*, 3779–3787. [[CrossRef](#)]
28. Zhang, X.; Dong, Y.; Gao, M.; Hao, M.; Ren, H.; Guo, L.; Guo, H. Knockdown of TRAP1 promotes cisplatin-induced apoptosis by promoting the ROS-dependent mitochondrial dysfunction in lung cancer cells. *Mol. Cell. Biochem.* **2020**, *476*, 1075–1082. [[CrossRef](#)]
29. Zaccara, S.; Ries, R.J.; Jaffrey, S.R. Reading, writing and erasing mRNA methylation. *Nat. Rev. Mol. Cell Biol.* **2019**, *20*, 608–624. [[CrossRef](#)]
30. Chassé, H.; Boulben, S.; Costache, V.; Cormier, P.; Morales, J. Analysis of translation using polysome profiling. *Nucleic Acids Res.* **2017**, *45*, e15. [[CrossRef](#)]
31. Oda, E.; Ohki, R.; Murasawa, H.; Nemoto, J.; Shibue, T.; Yamashita, T.; Tokino, T.; Taniguchi, T.; Tanaka, N. Noxa, a BH3-Only Member of the Bcl-2 Family and Candidate Mediator of p53-Induced Apoptosis. *Science* **2000**, *288*, 1053–1058. [[CrossRef](#)]
32. Xiang, Y.; Laurent, B.; Hsu, C.-H.; Nachtergaele, S.; Lu, Z.; Sheng, W.; Xu, C.; Chen, H.; Ouyang, J.; Wang, S.; et al. RNA m6A methylation regulates the ultraviolet-induced DNA damage response. *Nature* **2017**, *543*, 573–576. [[CrossRef](#)] [[PubMed](#)]
33. Shriwas, O.; Priyadarshini, M.; Samal, S.K.; Rath, R.; Panda, S.; Das Majumdar, S.K.; Muduly, D.K.; Botlagunta, M.; Dash, R. DDX3 modulates cisplatin resistance in OSCC through ALKBH5-mediated m6A-demethylation of FOXM1 and NANOG. *Apoptosis* **2020**, *25*, 233–246. [[CrossRef](#)] [[PubMed](#)]
34. Nie, S.; Zhang, L.; Liu, J.; Wan, Y.; Jiang, Y.; Yang, J.; Sun, R.; Ma, X.; Sun, G.; Meng, H.; et al. ALKBH5-HOXA10 loop-mediated JAK2 m6A demethylation and cisplatin resistance in epithelial ovarian cancer. *J. Exp. Clin. Cancer Res.* **2021**, *40*, 1–18. [[CrossRef](#)]
35. Tang, F.; Chen, L.; Gao, H.; Xiao, D.; Li, X. m6A: An Emerging Role in Programmed Cell Death. *Front. Cell Dev. Biol.* **2022**, *10*, 1–9. [[CrossRef](#)]
36. Meyer, K.D.; Patil, D.P.; Zhou, J.; Zinoviev, A.; Skabkin, M.A.; Elemento, O.; Pestova, T.V.; Qian, S.-B.; Jaffrey, S.R. 5' UTR m6A Promotes Cap-Independent Translation. *Cell* **2015**, *163*, 999–1010. [[CrossRef](#)] [[PubMed](#)]
37. Mao, Y.; Dong, L.; Liu, X.M.; Guo, J.; Ma, H.; Shen, B.; Qian, S.B. m6A in mRNA coding regions promotes translation via the RNA helicase-containing YTHDC2. *Nat. Commun.* **2019**, *10*, 1–11. [[CrossRef](#)]
38. Lin, S.; Choe, J.; Du, P.; Triboulet, R.; Gregory, R.I. The m6A Methyltransferase METTL3 Promotes Translation in Human Cancer Cells. *Mol. Cell* **2016**, *62*, 335–345. [[CrossRef](#)]
39. Ploner, C.; Kofler, R.; Villunger, A. Noxa: At the tip of the balance between life and death. *Oncogene* **2008**, *27*, S84–S92. [[CrossRef](#)]

-
40. Raj, N.; Wang, M.; Seoane, J.A.; Zhao, R.L.; Kaiser, A.M.; Moonie, N.A.; Demeter, J.; Boutelle, A.M.; Kerr, C.H.; Mulligan, A.S.; et al. The Mettl3 epitranscriptomic writer amplifies p53 stress responses. *Mol. Cell* **2022**, *82*, 2370–2384.e10. [[CrossRef](#)]
 41. Mojsa, B.; Lassot, I.; Desagher, S. Mcl-1 Ubiquitination: Unique Regulation of an Essential Survival Protein. *Cells* **2014**, *3*, 418–437. [[CrossRef](#)]